Unique diagram of a spatial arc and the knotting probability

Akio Kawauchi

Abstract. It is shown that the projection image of an oriented spatial arc to any oriented plane is approximated by a unique arc diagram (up to isomorphic arc diagrams) determined from the spatial arc and the projection. In a separated paper, the knotting probability of an arc diagram is defined as an invariant under isomorphic arc diagrams. By combining them, the knotting probability of every oriented spatial arc is defined.

1. Introduction

A *spatial arc* is a polygonal arc in the 3-space $\mathbf{R}^3$, which is considered as a model of a protein or a linear polymer in science. The following question on science is an interesting question that can be set as a mathematical question:

Question. How a linear scientific object such as a linear molecule (e.g. a non-circular DNA, protein, linear polymer,$\cdots$) is considered as a knot object ?

In this paper, it is shown that the projection image of an oriented spatial arc to any oriented plane is approximated into a unique arc diagrams (up to isomorphic arc diagrams) determined from the spatial arc and the projection. Further, the orientation change of the spatial arc makes only substitutes for these unique arc diagrams (up to isomorphic arc diagrams). This argument is more or less similar to an argument transforming a classical knot in $\mathbf{R}^3$ into a regular knot diagram (see [**1**], [**3**]). Let

$$S^2 = \{u \in \mathbf{R}^3 | \, ||u|| = 1\}$$

be the unit sphere, where $||\ ||$ denotes the norm on $\mathbf{R}^3$. Every element $u \in S^2$ is regarded as a unit vector from the origin 0. For a unit vector $u \in \mathbf{R}^3$, let P_u be the oriented plane containing the origin 0 such that the unit vector u is a positively normal vector to P_u. The orthogonal projection from $\mathbf{R}^3$ to the plane P_u is called the *projection along* the unit vector $u \in S^2$ and denoted by

$$\lambda_u : \mathbf{R}^3 \to P_u.$$

For a small positive number δ, a δ-*approximation* of the projection $\lambda_u : \mathbf{R}^3 \to P_u$ along $u \in S^2$ is the projection

$$\lambda_{u'} : \mathbf{R}^3 \to P_{u'}$$

2010 *Mathematics Subject Classification.* 57M25; 57Q45.

Key words and phrases. Arc diagram, Approximation, Spatial arc, Knotting probability.

along a unit vector $u' \in S^2$ with $||u' - u|| < \delta$, which is denoted by

$$\lambda_u^\delta : \mathbf{R}^3 \to P_u.$$

The projection image $\lambda_u(L)$ of a spatial arc L in the plane P_u is an *arc diagram* in the oriented plane P_u if $\lambda_u(L)$ has only *crossing points* (i.e., transversely meeting double points with over-under information) and the starting and terminal points as single points. The arc diagram $(P_u, \lambda_u(L))$ is sometimes denoted by (P, D).

An arc diagram (P, D) is *isomorphic* to an arc diagram (P', D') if there is an orientation-preserving homeomorphism $f : P \to P'$ sending D to D' which preserves the crossing points of D and D', and the starting and terminal points of D and D'. The map f is called an *isomorphism* from D to D'. In an illustration of an arc diagram, it is convenient to illustrate an arc diagram with smooth edges in the class of isomorphic arc diagrams instead of a polygonal arc diagram.

In this paper, the following observation is shown.

Theorem 1.1. Let L be an oriented arc in $\mathbf{R}^3$, and $\lambda_u : \mathbf{R}^3 \to P_u$ the projection along a unit vector $u \in S^2$. For any sufficiently small positive number δ, the projection λ_u has a δ-approximation

$$\lambda_u^\delta : \mathbf{R}^3 \to P_u$$

such that the projection image $\lambda_u^\delta(L)$ is an arc diagram determined uniquely from the spatial arc L and the projection λ_u up to isomorphic arc diagrams.

The proof of Theorem 1.1 is done in § 2. In [**10**], the knotting probability

$$p(D) = (p^{\mathrm{I}}(D), p^{\mathrm{II}}(D), p^{\mathrm{III}}(D))$$

of an arc diagram D is defined so that it is unique up to isomorphic arc diagrams. By the arc diagram $D(L; u) = \lambda_u^\delta(L)$, the *knotting probability* $p(L; u)$ of an oriented spatial arc L is defined by

$$p(L; u) = p(D(L; u))$$

for every unit vector $u \in S^2$. More details are discussed in § 3.

We mention here that a knotting probability of a circular knot is studied by Deguchi and Tsurusaki [**2**] (see also E. Uehara and T. Deguchi [**2**]) from the viewpoint of a random knotting, which is independent of our viewpoint. The case of a spatial arc is also studied by Millett, Dobay and Stasiak in [**12**] from a random knotting viewpoint with the same motivation as the present question[1]. We also note that a knotting probability of a spatial arc was defined directly from a knotting structure of a spatial graph but with the demerit that it depends on the heights of the crossing points of a diagram of the spatial arc in [**4, 6**].

In § 2, the proof of Theorem 1.1 is done. In § 3, the knotting probability of a spatial arc with a given direction of the projection is explained. In § 4, the knotting probability of an example of a spatial arc is computed.

[1]Some protein knotting data are listed in "KnotProt"(https://knotprot.cent.uw.edu.pl/).

2. Proof of Theorem 1.1

Let L be an oriented spatial arc, and s and p_t the starting point and the terminal point of L, respectively. The *front edge* of L is the interval γ in $\mathbf{R}^3$ joining the starting point s and the terminal point t. Orient γ by the orientation from s to t. Let $u(\gamma)$ be the unit vector of the front edge γ of L, called the *front edge vector* of L.

Let L be an oriented spatial arc with the starting point s and the terminal point t. An *edge line* of L is an oriented line[2] ℓ extending an edge of L oriented by L. The *front line* ℓ_γ is the oriented line extending the oriented front edge γ of L.

Assume that there is an edge line of L distinct from the front line ℓ_γ because otherwise there is nothing to show. The *starting front-pop line* of L is the edge line ℓ_s of the edge which pops for the first time from the front line ℓ_γ when a point is going on L along the orientation of L. The *ending front-pop line* of L is the edge line ℓ_t of the edge which reaches the front line ℓ_γ at the end when a point is going on L along the orientation of L.

The *starting front-pop plane* of an oriented spatial arc L is the oriented plane $P(\ell_\gamma, \ell_s)$ determined by the front line ℓ_γ and the starting pop line ℓ_s in this order. The *terminal front-pop plane* of an oriented spatial arc L is the oriented plane $P(\ell_\gamma, \ell_t)$ determined by the front line ℓ_γ and the terminal pop line ℓ_s in this order.

Let $u(\ell) \in S^2$ be the unit vector of an oriented line ℓ in $\mathbf{R}^3$. The unit vector $u(\ell_\gamma)$ of ℓ_γ is equal to the front edge vector $u(\gamma)$.

Let $u_s, u_t \in S^2$ denote the unit vectors $u(\ell_s)$ and $u(\ell_t)$ of the starting and terminal front-pop line ℓ_s and ℓ_t, called the *starting and terminal front-pop vectors*, respectively.

For a plane P in $\mathbf{R}^3$, the *great circle* C of P in S^2 is the great circle obtained as the intersection of S^2 and a plane P' parallel to P.

The *trace set* T of a spatial arc L is the subset of S^2 consisting of the great circles and the unit vectors obtained from L in the following cases (i) and (ii)*

(i) The great circle C of S^2 of the plane P in $\mathbf{R}^3$ determined by a vertex u of L and an edge line ℓ or the front line ℓ_γ of L which is disjoint from u.

(ii) The unit vectors $\pm u_\eta \in S^2$ of an oriented line η in $\mathbf{R}^3$ meeting three edge lines $\ell_i\,(i = 1, 2, 3)$ of L any two of which are not on the same plane with 3 distinct points.

By (i), note that the following great circles are in the trace set T:

(1) the great circles of the starting and terminal front-pop planes $P(\ell_\gamma, \ell_s)$ and $P(\ell_\gamma, \ell_t)$,

(2) the great circle of the plane determined by two parallel distinct edge lines $\ell and \ell'$,

(3) the great circle of the plane determined by two distinct edge lines ℓ, ℓ' meeting a point,

(4) the great circle of the plane determined by an edge line ℓ and the front line ℓ_γ meeting a point.

[2]Throughout the paper, by a *line*, we mean a straight line in $\mathbf{R}^3$.

In particular, the unit vectors $\pm u(\ell) \in S^2$ of every edge line ℓ of L and the unit vectors $\pm u(\ell_\gamma) \in S^2$ and the great circle of any plane containing any three distinct lines $\ell_i\,(i = 1, 2, 3)$ is the trace set T. Also the unit vectors $\pm u(\eta) \in S^2$ of an oriented line η in $\mathbf{R}^3$ meeting three edge lines $\ell_i\,(i = 1, 2, 3)$ of L some two of which are on the same plane with 3 distinct points.

In (ii), note that a line η meeting $\ell_i\,(i = 1, 2, 3)$ by different 3 points is unique, because if there is another such line η', then the lines $\eta, \eta', \ell_i\,(i = 1, 2, 3)$ and hence the lines $\ell_i\,(i = 1, 2, 3)$ are on the same plane, contradicting the assumption.

Also, note that if a unit vector $u \in S^2$ is in the trace set T, then $-u$ is also in T.

For every unit vector $u \in S^2$, let P_u be the oriented plane containing the origin 0 such that u is positively normal to P_u, and $\lambda_u : \mathbf{R}^3 \to P_u$ the orthogonal projection. We show the following lemma.

Lemma 2.1. For every unit vector $u \in S^2 \setminus T$, the projection image $\lambda_u(L)$ is an arc diagram in the plane P_u. Further, the arc diagram $\lambda_u(L)$ up to isomorphic arc diagrams is independent of any choice of a unit vector u' in the connected region $R(u)$ of $S^2 \setminus T$ containing u.

Proof of Lemma 2.1. If a unit vector $u \in S^2$ is not in (i), then every edge of L and the front line ℓ_γ are embedded in the plane P_u by the projection λ_u. If a unit vector $u \in S^2$ is in neither (i) nor (ii), then the set of vertexes of L is embedded in P_u by the projection λ_u whose image is disjoint from the image of any open edge of L. In particular, any two distinct parallel edge lines are disjointedly embedded in P_u. Further, the images of the edges of L meet only in the images of the open edges of L. Thus, if a unit vector $u \in S^2$ is in neither (i) nor (ii), namely if $u \in S^2 \setminus T$, then the meeting points among the edges of L consisting of double points between two open edges of L and hence the projection image $\lambda_u(L)$ is an arc diagram in the plane P_u. The arc diagram $\lambda_{u'}(L)$ is unchanged up to isomorphisms for any unit vector u' in a connected open neighborhood of u in $S^2 \setminus T$, so that the arc diagram $\lambda_{u'}(L)$ is unchanged up to isomorphisms for any unit vector u' in the connected region $R(u)$. □

The proof of Theorem 1.1 is done as follows:

Proof of Theorem 1.1. The idea of the proof is to specify a unique connected region $R(u')$ of $S^2 \setminus T$ adjacent to every unit vector $u \in S^2$. For this purpose, for any given oriented spatial arc L (not in the front line ℓ_γ), the new x-axis, y-axis and z-axis of the 3-space $\mathbf{R}^3$ are set as follows:

The front edge vector $u(\gamma)$ of the front edge γ is taken as the unit vector of the x-axis and denoted by u_x:

$$u(\gamma) = u_x = (1, 0, 0).$$

Let $u_y \in S^2$ be the unit vector orthogonal to the front edge vector $u_x = u(\gamma)$ in the starting front-pop plane $P(\ell_\gamma, \ell_s)$ of L with positive inner product $u_y \cdot u_s$ for the starting front-pop vector u_s. The unit vector u_y is taken as the unit vector the y-axis:

$$u_y = (0, 1, 0).$$

Then the exterior product $u_z = u_x \times u_y$ is given by the z-axis:

$$u_z = (0, 0, 1).$$

Note that the unit vectors u_x, u_y, u_z are uniquely specified by the oriented spatial arc L.

Under this setting of the coordinate axis, let S^2 be the unit sphere which is the union of the upper hemisphere S^2_+, the equatorial circle S^2_0 and the lower hemisphere S^2_- given as follows:

$$\begin{aligned} S^2_+ &= \{(x, y, z) \in \mathbf{R}^3 | \, x^2 + y^2 + z^2 = 1, \, z > 0\}, \\ S^2_0 &= \{(x, y, z) \in \mathbf{R}^3 | \, x^2 + y^2 + z^2 = 1, \, z = 0\}, \\ S^2_- &= \{(x, y, z) \in \mathbf{R}^3 | \, x^2 + y^2 + z^2 = 1, \, z > 0\}. \end{aligned}$$

Note that the equatorial circle S^2_0 belongs to T since the front-pop plane P_L coincides with the plane with $z = 0$.

Every unit vector u in S^2_+ except the north pole $(0, 0, 1)$ is uniquely written as

$$u = \psi(r, \theta) = (r \cos\theta, r \sin\theta, \sqrt{1 - r^2})$$

for real numbers r and θ with $0 < r \leq 1$ and $0 \leq \theta < 2\pi$ in a unique way.

Case 1: $u = \psi(r, \theta) \in S^2_+$ with $0 < r < 1$.

Note that when the number r with $0 < r < 1$ is fixed, the points $\psi(r, \theta')$ for all θ' with $0 \leq \theta' < 2\pi$ form a circle in S^2 which is different from every great circle of S^2 and hence meets T only in finitely many points.

The connected region $R(u')$ is taken to be the connected region of $S^2_+ \setminus T$ which is adjacent to the unit vector $\psi(r, \theta')$ and contains the unit vector $\psi(r, \theta + \varepsilon)$ for a sufficiently small positive number ε, which is uniquely determined.

Case 2: $u = (0, 0, 1) \in S^2_+$. By taking a positive number r sufficiently small, take a unit vector $\psi(r, 0) = (r, 0, \sqrt{1 - r^2}) \in S^2_+$ such that $\psi(r', 0)$ does not meet the great circles in T for any r' with $0 < r' \leq r$ except for the meridian circle $x^2 + z^2 = 1$ (if it is in T). Then the connected region $R(u')$ is taken to be the connected region of $S^2_+ \setminus T$ which is adjacent to the unit vector $\psi(r, 0)$ and contains the unit vector $\psi(r, \varepsilon)$ for a sufficiently small positive number ε, which is uniquely determined.

Case 3: $u = \psi(1, \theta) \in S^2_0$.

Let $0 \leq \theta < \pi$. By taking a positive number r with $1 - r$ a sufficiently small positive number, take a unit vector $\psi(r, \theta) \in S^2_+$ such that $\psi(r', \theta)$ does not meet the great circles in T for any r' with $r \leq r' < 1$. Then the connected region $R(u')$ is taken to be the connected region of $S^2_+ \setminus T$ which is adjacent to the unit vector $\psi(r, \theta)$ and contains the unit vector $\psi(r, \theta + \varepsilon)$ for a sufficiently small positive number ε, which is uniquely determined.

Let $\pi \leq \theta < 2\pi$. Since $-u = \psi(1, \theta - \pi) \in S^2_0$, we specified the connected component $R((-u)')$ of $S^2 \setminus T$. The desired connected component $R(u')$ of $S^2 \setminus T$ is the image of $R((-u)')$ under the antipodal map $-1 : S^2 \to S^2$ defined by (x, y, z) to $(-x, -y, -z)$ with $(-1)(T) = T$.

Case 4: $u \in S^2_-$.

Since the unit vector $-u$ is in S^2_+, we specified the connected component $R((-u)')$ of $S^2 \setminus T$ in the cases 1-3. The desired connected component $R(u')$ of $S^2 \setminus T$ is the image of $R(u')$ under the antipodal map $-1 : S^2 \to S^2$.

Thus, for every unit vector $u \in S^2$, the connected region $R(u')$ and is specified, so that for every $u'' \in R(u')$, the image $\lambda_{u''}(L)$ of L by the orthogonal projection $\lambda_{u''} : \mathbf{R}^3 \to P_{u''}$ is an arc diagram determined uniquely up to isomorphic arc diagrams from L and the projection λ_u.

Since the connected region $R(u')$ is adjacent to the normal vector $u \in S^2$, for every $\delta > 0$ there is a unit vectors $u'' \in R(u')$ with $||u'' - u'|| < \delta$ and by Lemma 3.1, the orthogonal projection $\lambda_{u''} : \mathbf{R}^3 \to P_{u''}$ is a desired δ-approximation $\lambda_u^\delta : \mathbf{R}^3 \to P_u$. This completes the proof of Theorem 1.1. □

An arc diagram D is *inbound* if the starting point s and the terminal point t of D are in the same region of the plane divided by the arc diagram D. More generally, the projection image $\lambda_u(L)$ of a spatial arc L which need not be an arc diagram is *inbound* if

$$\lambda_u(L \setminus \partial\gamma) \cap \lambda_u(\gamma) = \emptyset$$

for the front edge γ of L. A spatial arc L is an *arc knot* if the union $\mathrm{cl}(L) = \bar{L} = L \cup \gamma$ of L and the front edge γ of L is a knot (i.e., a simple closed curve) in $\mathbf{R}^3$. The knot $\mathrm{cl}(L)$ is called the *closed knot* of L. A spatial arc L is *even* if the starting front-pop plane $P(\ell_\gamma, \ell_s)$ and the terminal front-pop plane $P(\ell_\gamma, \ell_t)$ are exactly the same. Let $-L$ denote the same spatial arc as L but with the opposite orientation. We have the following observations from the proof of Theorem 1.1.

Corollary 2.2. For an oriented spatial arc L and an arc diagram $D(L; u) = \lambda_u^\delta(L)$, we have the following (1)-(5).

(1) The arc diagram $D(L; -u)$ is the mirror image of $D(L; u)$.

(2) If the projection image $\lambda_u(L)$ is an arc diagram, then the arc diagram $D(L; u)$ is isomorphic to the arc diagram $\lambda_u(L)$.

(3) There are only finitely many arc diagrams $D(L; u)$ up to isomorphic arc diagrams for all unit vectors $u \in S^2$.

(4) If the projection image $\lambda_u(L)$ is inbound, then the arc diagram $D(L; u)$ is an inbound arc diagram. In particular, if L is an arc knot, then the arc diagram $D(L; u_x)$ for the front edge vector u_x is an inbound arc diagram.

(5) If the spatial arc L is even, then the arc diagram $D(-L; u)$ is isomorphic to the arc diagram $D(L; u)$ or the mirror image $D(L; -u)$ of $D(L; u)$ with the string orientation changed according to whether the orientations of $P(\ell_\gamma, \ell_s)$ and $P(\ell_\gamma, \ell_t)$ coincide or not.

3. The knotting probability of a spatial arc

A *chord graph* is a trivalent connected graph $(o; \alpha)$ in $\mathbf{R}^3$ consisting of a trivial oriented link o (called a *based loop system*) and the attaching arcs α (called a it chord system), where some chords of α may meet. A *chord diagram* is a diagram $C(o; \alpha)$ (in a plane) of a chord graph $(o; \alpha)$.

A *ribbon surface-link* is a surface-link in the 4-space $\mathbf{R}^4$ obtained from a trivial S^2-link by mutually disjoint embedded 1-handles (see [**11**, II], [**14**]). From a chord diagram C, a ribbon surface-link $F(C)$ in the 4-space $\mathbf{R}^4$ is constructed so that an

equivalence of $F(C)$ corresponds to a combination of the moves M_0, M_1 and M_2 (see [**5, 7, 8, 9**]).

Let D be an oriented n-crossing arc diagram. We obtain from D a chord diagram $C(D)$ with $n+2$ based loops and n chords by replacing every crossing point and every endpoint with a based loop as in Fig. 1.

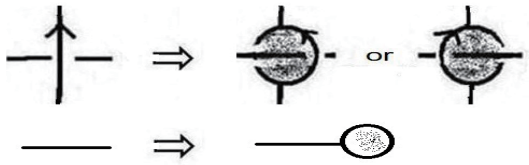

FIGURE 1. Transformation of an oriented arc diagram into a chord diagram

Let D be an oriented n-crossing arc diagram, and $C(D)$ the chord diagram of D. Let o_s and o_t be the based loops in $C(D)$ transformed from the starting and terminal points v_s and v_t, respectively. There are $(n+2)^2$ chord diagrams A obtained from the chord diagram $C(D)$ by joining the loops o_s and o_t with any based loops of $C(D)$ by two chords not passing the other based loops. A chord diagram obtained in this way is called an adjoint chord diagram of $C(D)$ with an *additional chord pair*. Note that the ribbon surface-knot $F(C(D))$ of the chord diagram $C(D)$ is a ribbon S^2-knot and the ribbon surface-knot $F(A)$ of an adjoint chord diagram A is a genus 2 ribbon surface-knot. A chord diagram is said to be *unknotted* or *knotted* according to whether it represents a trivial or non-trivial ribbon surface-knot, respectively.

The idea of the knotting probability is to measure how many knotted chord diagrams there are among the $(n+2)^2$ adjoint chord diagrams of $C(D)$. Since there are canonical overlaps among them up to canonical isomorphisms, we consider the n^2+2n+2 adjoint chord diagrams A of $C(D)$ by removing them which are classified by the following three types:

Type I. Here are the 2 adjoint chord diagrams of $C(D)$ which are the adjoint chord diagram with two self-attaching additional chords and the adjoint chord diagram with a self-attaching additional chord on o_s and an additional chord joining o_s with o_t.

Type II. Here are the $2n$ adjoint chord diagrams A of $C(D)$. The $2n$ adjoint chord diagrams of $C(D)$ are given by the additional chord pairs consist of a self-attaching additional chord on o_s (or o_t, respectively) and an additional chord joining o_t (or o_s, respectively) with a based loop except for o_s and o_t.

Type III. Here are the n adjoint chord diagrams A of $C(D)$ where the additional chord pairs consist of an additional chord joining o_s with o_t and an additional chord joining o_s with a a based loop except for o_s and o_t.

Type IV. Here are the $n(n-1)$ adjoint chord diagrams A of $C(D)$ where the additional chord pair joins the pair of o_s and o_t with a distinct based loop pair not containing o_s and o_t.

In [**10**], it is shown that every adjoint chord diagram of the chord diagram $C(D)$ of any n crossing arc diagram D is deformed into one of the adjoint chord diagrams of type I, II, III and IV of the chord diagram $C(D)$. Thus, it is justified to reduce the $(n+2)^2$ adjoint chord diagrams to the n^2+2n+2 adjoint chord diagrams.

The *knotting probability* $p(D)$ of an arc diagram D is defined to be the quadruplet

$$p(D) = (p^{\mathrm{I}}(D), p^{\mathrm{II}}(D), p^{\mathrm{III}}(D), p^{\mathrm{IV}}(D))$$

of the following knotting probabilities $p^{\mathrm{I}}(D)$, $p^{\mathrm{II}}(D)$, $p^{\mathrm{III}}(D)$, $p^{\mathrm{IV}}(D)$ of types I, II III, IV.

Definition.
(1) Let A_1 and A_2 be the adjoint chord diagrams of type I and assume that there are just k knotted chord diagrams among them. Then the *type I knotting probability* of D is

$$p^{\mathrm{I}}(D) = \frac{k}{2}.$$

Thus, $p^{\mathrm{I}}(D)$ is $0, \frac{1}{2}$ or 1 for any arc diagram D.

(2) Let $A_i\,(i = 1, 2, \ldots, 2n)$ be the adjoint chord diagrams of type II and assume that there are just k knotted chord diagrams among them. Then the *type II knotting probability* of D is

$$p^{\mathrm{III}}(D) = \frac{k}{2n}.$$

(3) Let $A_i\,(i = 1, 2, \ldots, n)$ be the adjoint chord diagrams of type III and assume that there are just k knotted chord diagrams among them. Then the *type III knotting probability* of D is

$$p^{\mathrm{III}}(D) = \frac{k}{n}.$$

(4) Let $A_i\,(i = 1, 2, \ldots, n(n-1))$ be the adjoint chord diagrams of type IV and assume that there are just k knotted chord diagrams among them. Then the *type IIV knotting probability* of D is

$$p^{\mathrm{IV}}(D) = \frac{k}{n(n-1)}.$$

When the orientation of an arc diagram D is changed, all the orientations of the based loops of the chord graph $C(D)$ are changed at once. This means that the knotting probability $p(D)$ does not depend on any choice of orientations of D, and we can omit the orientation of D in figures. See [**10**] for actual calculations of $p(D)$. It is known by [**10**, Theorem 3.3 (3)] that $p^{\mathrm{I}}(D) = 0$ or 1, $p^{\mathrm{II}}(D) = p^{\mathrm{III}}(D)$ and $p(D) = p(D^*)$ for any inbound arc diagram D and the mirror image D^* of D.

The knotting probability $p(D)$ has $p(D) = 1$ if

$$p^{\mathrm{I}}(D) = p^{\mathrm{II}}(D) = p^{\mathrm{III}}(D) = p^{\mathrm{IV}}(D) = 1$$

and otherwise, $p(D) < 1$. The knotting probability $p(D)$ has $p(D) > 0$ if

$$p^{\mathrm{I}}(D) + p^{\mathrm{II}}(D) + p^{\mathrm{III}}(D) + p^{\mathrm{IV}}(D) > 0$$

and otherwise, $p(D) = 0$.

For an oriented spatial arc L in $\mathbf{R}^3$, the *knotting probability* $p(L;u)$ of L for a unit vector $u \in S^2$ is defined to be

$$p(L;u) = p(D(L;u))$$

for the arc diagram $D(L;u)$ for u. Thus,

$$\begin{aligned} p^{\mathrm{I}}(L;u) &= p^{\mathrm{I}}(D(L;u)), \\ p^{\mathrm{II}}(L;u) &= p^{\mathrm{II}}(D(L;u)), \\ p^{\mathrm{III}}(L;u) &= p^{\mathrm{III}}(D(L;u)), \\ p^{\mathrm{IV}}(L;u) &= p^{\mathrm{IV}}(D(L;u)). \end{aligned}$$

Although $p(L;u)$ is unchanged by any choice of a string orientation in the arc diagram level $D(L;u)$, the knotting probability $p(-L;u)$ may be much different from the arc diagram $p(L;u)$ in general, because the arc diagram $D(L;u)$ may be much different from the arc diagram $D(-L;u)$ in general (cf. Corollary 2.4). In any case, the unordered pair of $p(L;u)$ and $p(-L;u)$ is considered as the knotting probability of a spatial arc L independent of the string orientation. When one-valued probability is desirable, a suitable average of the knotting probabilities

$$p^{\mathrm{I}}(\pm L;u),\ p^{\mathrm{II}}(\pm L;u),\ p^{\mathrm{III}}(\pm L;u),\ p^{\mathrm{IV}}(\pm L;u)$$

is considered. For a special spatial arc L, we have the following corollary.

Corollary 3.1.
(1) If the projection image $\lambda_u(L)$ is inbound, then

$$p(L;u) = p(L;-u).$$

In particular, if L is an arc knot, then $p(L;u_x) = p(L;-u_x)$ for the front edge vector u_x.

(2) If L is even, then

$$p(-L;u) = p(L;u) \quad \text{or} \quad p(-L;u) = p(L;-u)$$

for any unit vector $u \in S^2$ according to whether the orientations of $P(\ell_\gamma, \ell_s)$ and $P(\ell_\gamma, \ell_t)$ coincide or not.

(3) If L is even and the projection image $\lambda_u(L)$ is inbound, then the four knotting probabilities $p(\pm L;\pm u)$ are equal to $p(L;u)$.

Proof of Corollary 3.1. In [**10**], it is shown $p(D) = p(D^*)$ for an inbound arc diagram D and the mirror image D^* of D. By Corollary 2.2 (1) and (4), the arc diagrams $D(L;u)$ and $D(L;u_x)$ are inbound arc diagram with $D(L;-u)$ and $D(L;-u_x)$ the mirror images. Thus, (1) is obtained. For (2), by Corollary 2.2 (1) and (5), the arc diagram $D(-L;u)$ is isomorphic to the arc diagram $D(L;u)$ or $D(L;-u)$ according to whether the orientations of $P(\ell_\gamma, \ell_s)$ and $P(\ell_\gamma, \ell_t)$ coincide or not. The assertion (3) is a combination result of (1) and (2). □

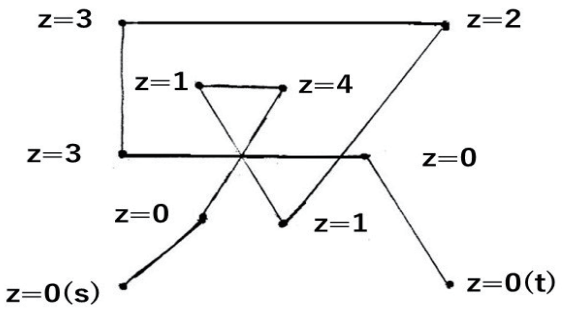

FIGURE 2. The spatial arc L given by the vertex coordinate data: namely, the (x, y) vertex coordinates $(0,0),(1,1),(2,3),(1,3),(2,1),(4,4),(0,4),(0,2),(3,2),(4,0)$ of $\lambda_{u_z}(L)$ in the xy plane and the z vertex coordinate data in the figure.

4. Computing some examples

It is stated in Corollary 2.2 (3) that for every spatial arc L, there are only finitely many arc diagrams $D(L;u)$ up to isomorphic arc diagrams for all unit vectors $u \in S^2$. However, it is a very hard problem to enumerate all the arc diagrams $D(L;u)$ even for a simple spatial arc L. By this reason and Corollary 3.1, at most the 12 arc diagrams $D(\pm L;\pm u_x)$, $D(\pm L;\pm u_y)$ and $D(\pm L;\pm u_z)$ determined uniquely by the spatial arc L are recommended in computing the knotting probabilities for an actual spatial arc.

In this section, the knotting probabilities of three concrete examples of even arc knots are computed in Examples A, B and C.

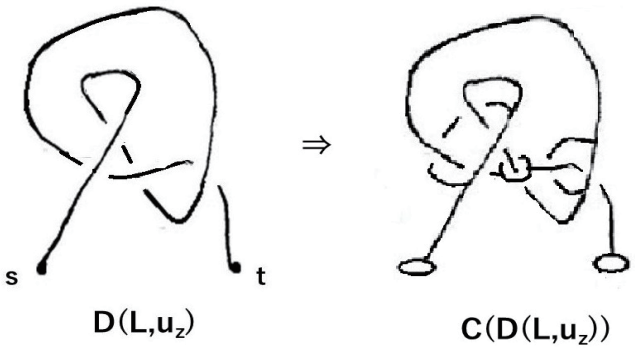

FIGURE 3. Producing the chord diagram $C(D(L;u_z))$ and a simplified chord diagram from the projection image $\lambda_{u_z}(L)$

Example A. Consider an even arc knot L in Fig. 2 given by the projection image $\lambda_{u_z}(L)$ in the xy plane together with z-coordinate information such that the vertex coordinates $(x, y)^z$ of L ordered from the starting point s are given by

$$(0,0)^0, (1,1)^0, (2,3)^4, (1,3)^1, (2,1)^1, (4,4)^2, (0,4)^3, (0,2)^3, (3,2)^0, (4,0)^0.$$

The closed knot $\mathrm{cl}(L)$ is a trefoil knot. The arc diagram $D(L; u_z)$ obtained from $\lambda_{u_z}(L)$ is illustrated in Fig. 3. In computing the knotting probability $p(L; u_z)$ from the chord diagram $C(D(L; u_z))$ of the arc diagram $D(L; u_z)$, a simplified chord diagram of the chord diagram $C(D(L; u_z))$ given by the following observation is used to make the computation simpler.

Observation 4.1. If two based loops are connected by a chord not meeting the other chords, one can replace the two based loops with the chord by one based loop without changing the knotting probability.

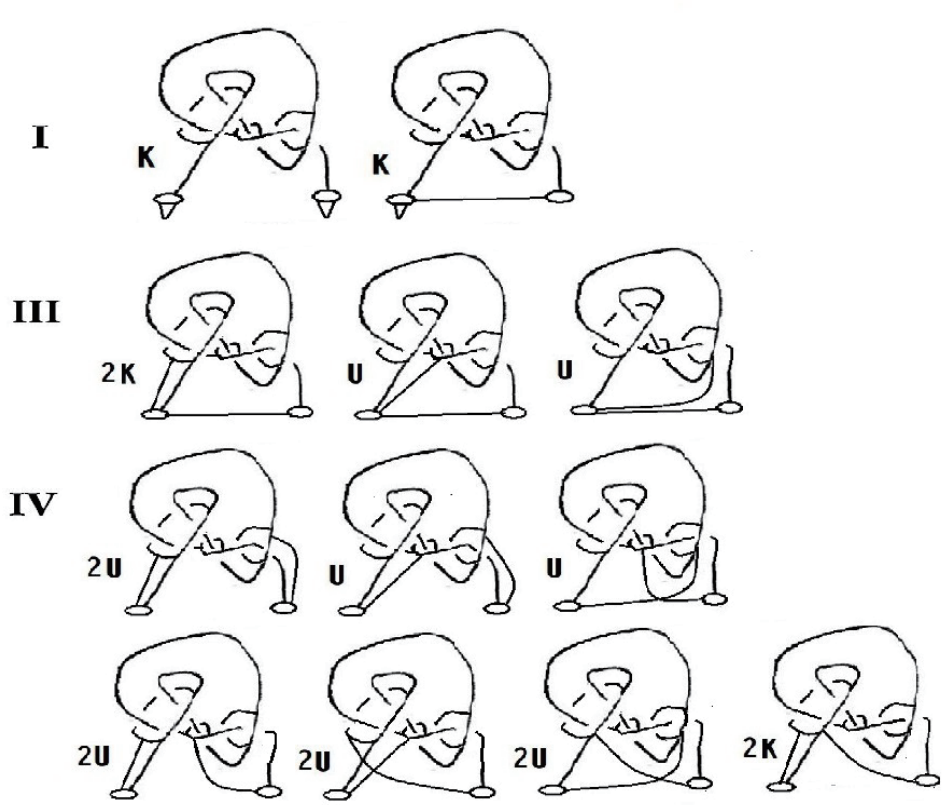

FIGURE 4. Calculations on the chord diagram $C(D(L; u_z))$

In Fig. 3, a simplified chord diagram of the chord diagram $C(D(L; u_z))$ is given. In the use of a simplified chord diagram obtained by using Observation 4.1, a

carefulness is needed in counting the knotted and unknotted adjoint chord diagrams. In fact, a calculation on the numbers of the knotted and unknotted adjoint chord diagrams of the arc diagram $C(D(L;u_z))$ using the simplified chord diagram of $C(D(L;u_z))$ is done in Fig. 4 (see [**10**] for the details of the calculation). Thus, we have

$$p(L;u_z) = p(L;-u_z) = p(-L,u_z) = p(-L,-u_z) = (1, \frac{1}{2}, \frac{1}{2}, \frac{1}{6})$$

by Corollary 3.1, for L is an even spatial arc and $D(L;u_z)$ is an inbound arc diagram.

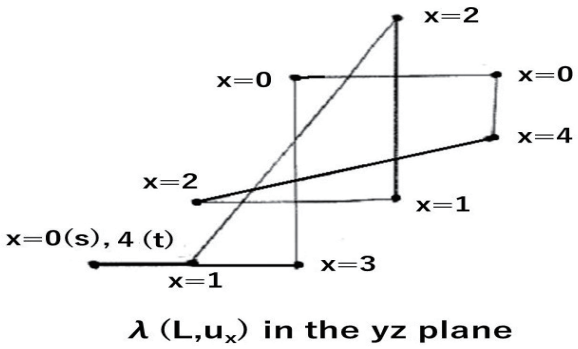

FIGURE 5. The spatial arc L given by the vertex coordinate data: namely, the (y,z) vertex coordinates $(0,0),(1,0),(3,4),(3,1),(1,1),(4,2),(4,3),(2,3),(2,0),(0,0)$ of $\lambda_{u_x}(L)$ in the yz plane and the x vertex coordinate data in the figure.

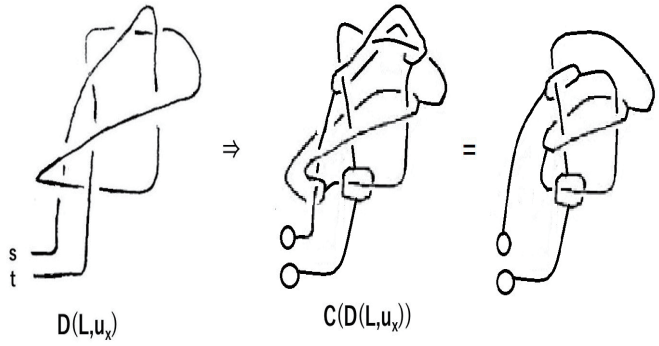

FIGURE 6. Producing the chord diagram $C(D(L;u_x))$ and a simplified chord diagram from the projection image $\lambda_{u_x}(L)$

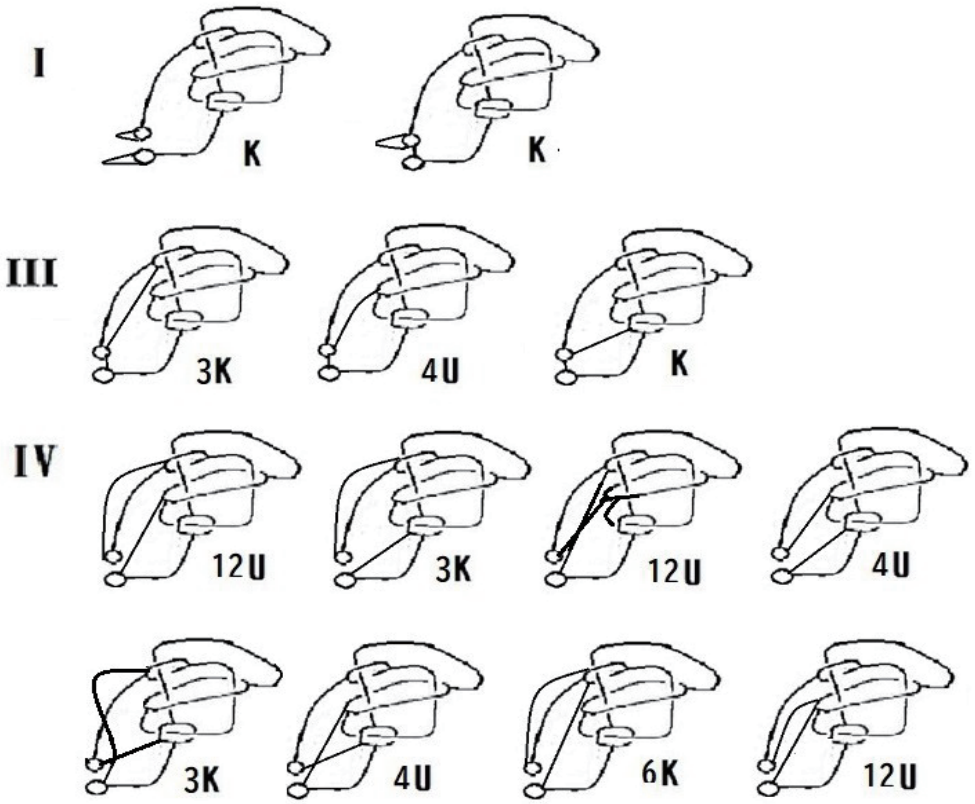

FIGURE 7. Calculations on the chord diagram $C(D(L;u_x))$

In Fig. 5, the same arc knot L is presented by the projection image $\lambda_{u_x}(L)$ in the yz plane together with x-coordinate information such that the vertex coordinates $(y,z)^x$ of L ordered from the starting point s are given by

$$(0,0)^0,(1,0)^1,(3,4)^2,(3,1)^1,(1,1)^2,(4,2)^4,(4,3)^0,(2,3)^0,(2,0)^3,(0,0)^4.$$

The arc diagram $D(L;u_x)$ obtained from $\lambda_{u_x}(L)$ is illustrated in Fig. 6. In Fig. 6, the chord diagram $C(D(L;u_x))$ and a simplified chord diagram of it are illustrated. A calculation on the numbers of the knotted and unknotted adjoint chord diagrams of the arc diagram $C(D(L;u_x))$ using the simplified chord diagram of $C(D(L;u_x))$ is done in Fig. 7. Thus, we have

$$p(L;u_x)=p(L;-u_x)=p(-L,u_x)=p(-L,-u_x)=(1,\frac{1}{2},\frac{1}{2},\frac{3}{14})$$

by Corollary 3.1, for L is an even arc knot and $D(L;u_x)$ is an inbound arc diagram.

In Fig. 8, the same arc knot L is presented by the projection image $\lambda_{u_y}(L)$ in the zx plane together with y-coordinate information such that the vertex coordinates

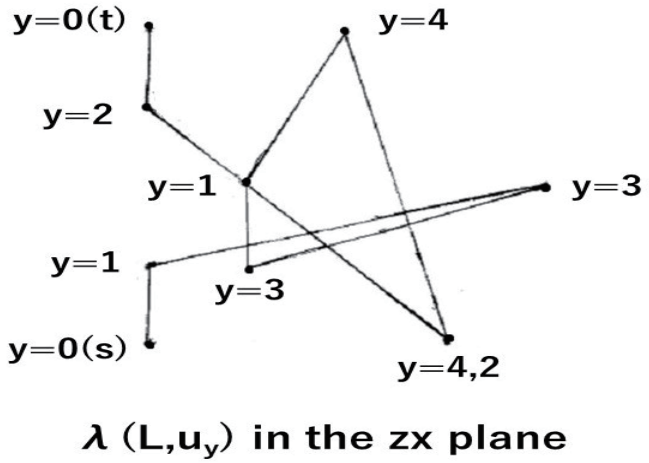

FIGURE 8. The spatial arc L given by the vertex coordinate data: namely, the (y, z) vertex coordinates $(0,0), (0,1), (4,2), (1,1), (1,2), (2,4), (3,0), (3,0), (0,3), (0,4)$ of $\lambda_{u_y}(L)$ in the yz plane and the y vertex coordinate data in the figure.

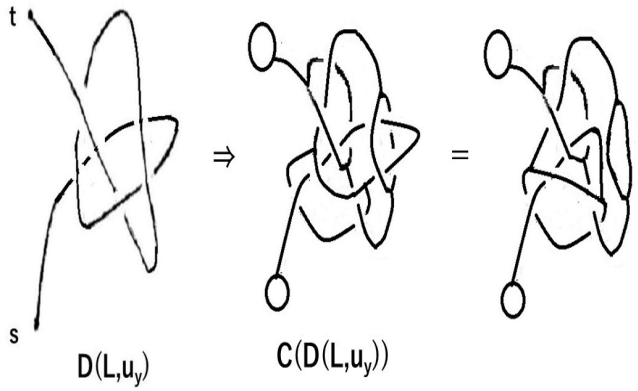

FIGURE 9. Producing the chord diagram $C(D(L; u_y))$ and a simplified chord diagram from the projection image $\lambda_{u_y}(L)$

$(z, x)^y$ of L ordered from the starting point s are given by

$$(0,0)^0, (0,1)^1, (4,2)^3, (1,1)^3, (1,2)^1, (2,4)^4, (3,0)^4, (3,0)^2, (0,3)^2, (0,4)^0.$$

The arc diagram $D(L; u_y)$ obtained from $\lambda_{u_y}(L)$ is illustrated in Fig. 9. In Fig. 9, the chord diagram $C(D(L; u_y))$ and a simplified chord diagram of it are illustrated. A calculation on the numbers of the knotted and unknotted adjoint chord diagrams of the arc diagram $C(D(L; u_y))$ using the simplified chord diagram of $C(D(L; u_y))$

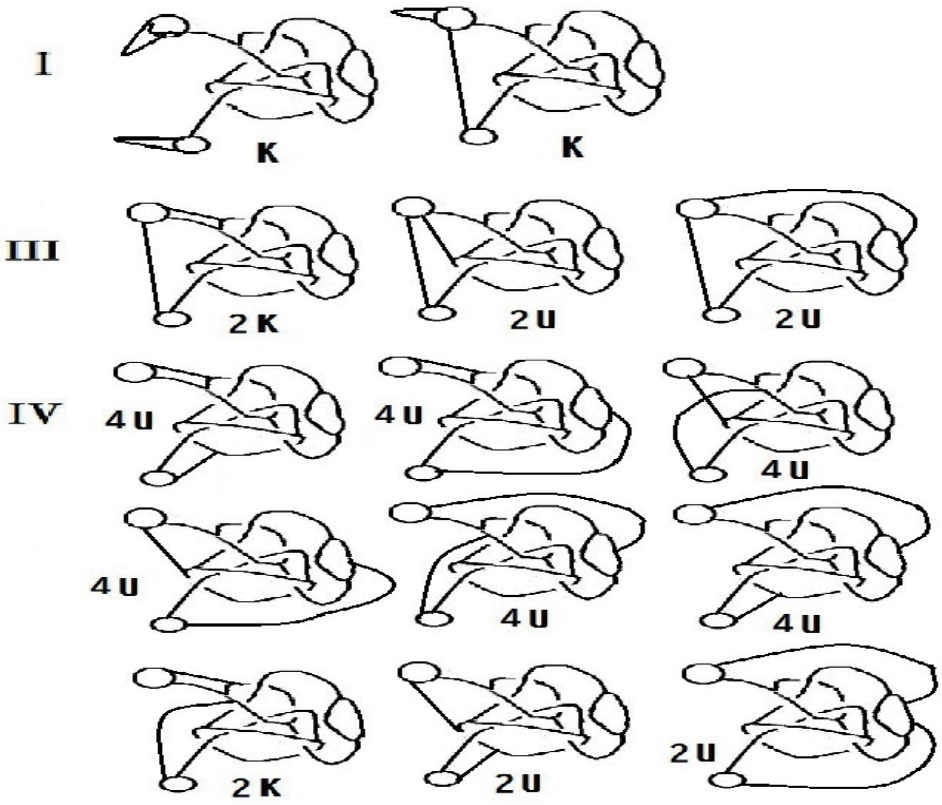

FIGURE 10. Calculations on the chord diagram $C(D(L;u_y))$

is done in Fig. 10. Thus, we have

$$p(L;u_y) = p(L;-u_y) = p(-L,u_y) = p(-L,-u_y) = (1,\frac{1}{2},\frac{1}{2},\frac{1}{15})$$

by Corollary 3.1, for L is an even arc knot and $D(L;u_y)$ is an inbound arc diagram.

Example B. Consider an even arc knot L in Fig. 11 given by the non-inbound projection image $\lambda_{u_z}(L)$ in the xy plane together with z-coordinate information such that the vertex coordinates $(x,y)^z$ of L ordered from the starting point s are given by

$$(0,0)^0,(1,1)^0,(2,3)^1,(3,1)^{-1},(1,-1)^2,(-1,0)^1,(1,2)^0,(3,0)^0.$$

The closed knot $\mathrm{cl}(L)$ is also a trefoil knot. The knotting probability of the chord diagrams $C(D(L;\pm u_z))$ of the arc diagrams $D(L;\pm u_z)$ has been computed in [**10**]. Thus, we have

$$p(L;u_z) = p(-L,-u_z) = (\frac{1}{2},\frac{1}{2},0,\frac{1}{2}), \quad p(L;-u_z) = p(-L,u_z) = 0.$$

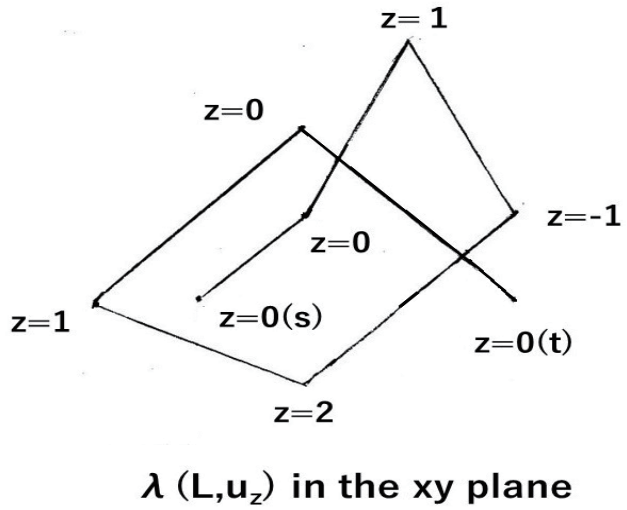

FIGURE 11. The spatial arc L given by the vertex coordinate data: namely, the (x, y) vertex coordinates $(0, 0), (1, 1), (2, 3), (3, 1), (1, -1), (-1, 0), (1, 2), (3, 0)$ of $\lambda_{u_z}(L)$ in the xy plane and the z vertex coordinate data in the figure.

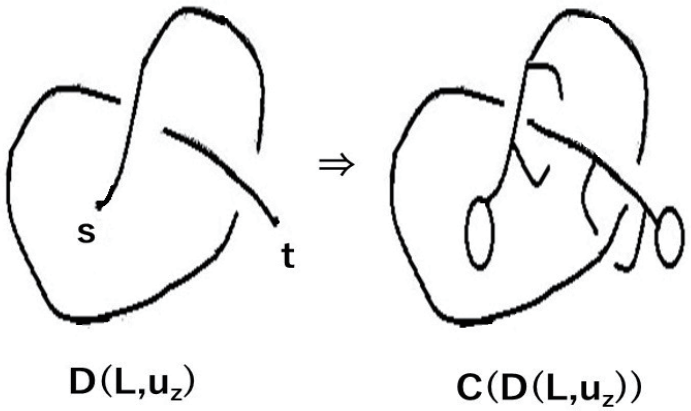

FIGURE 12. Producing the arc diagram $D(L; u_z)$ and the chord diagram $C(D(L; u_z))$.

In Fig. 13, the same arc knot L is presented by the projection image $\lambda_{u_x}(L)$ in the yz plane together with x-coordinate information such that the vertex coordinates $(y, z)^x$ of L ordered from the starting point s are given by

$$(0, 0)^0, (1, 0)^1, (3, 1)^2, (1, -1)^3, (-1, 2)^1, (0, 1)^{-1}, (2, 0)^1, (0, 0)^3.$$

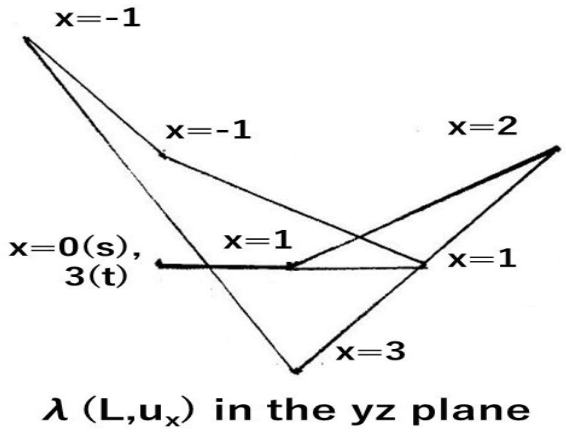

FIGURE 13. The spatial arc L given by the vertex coordinate data: namely, the (y, z) vertex coordinates $(0,0),(1,0),(3,1),(1,-1),(-1,2),(0,1),(2,0),(0,0)$ of $\lambda_{u_x}(L)$ in the yz plane and the x vertex coordinate data in the figure.

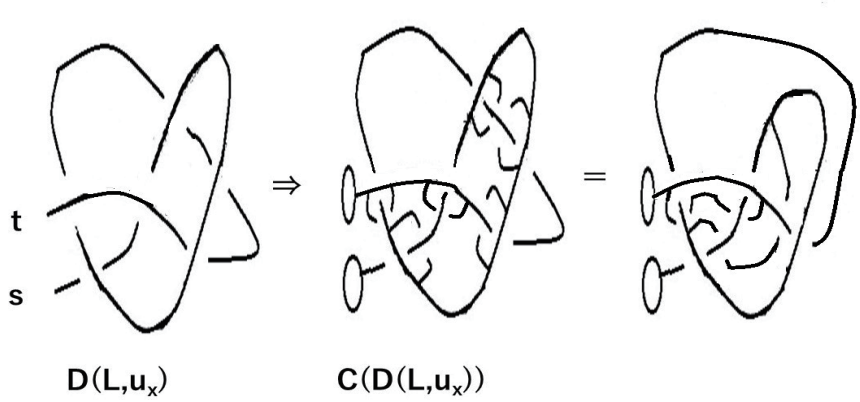

FIGURE 14. Producing the chord diagram $C(D(L;u_x))$ and a simplified chord diagram from the projection image $\lambda_{u_x}(L)$

The arc diagram $D(L;u_x)$ obtained from $\lambda_{u_x}(L)$ is illustrated in Fig. 14. In Fig. 14, the chord diagram $C(D(L;u_x))$ and a simplified chord diagram of it are illustrated. A calculation on the numbers of the knotted and unknotted adjoint chord diagrams of the arc diagram $C(D(L;u_x))$ using the simplified chord diagram of $C(D(L;u_x))$ is done in Fig. 15. Thus, we have

$$p(L;u_x) = p(L;-u_x) = p(-L,u_x) = p(-L,-u_x) = (1, \frac{1}{3}, \frac{1}{3}, \frac{1}{15})$$

by Corollary 3.1, for L is an even arc knot and $D(L;u_x)$ is an inbound chord diagram.

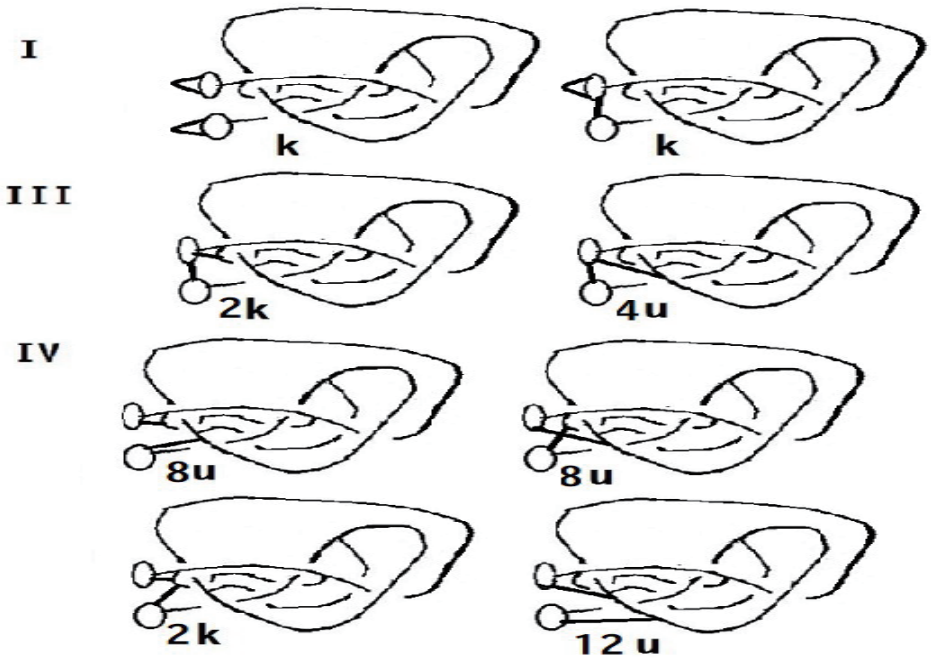

FIGURE 15. Calculations on the chord diagram $C(D(L;u_x))$

In Fig. 16, the same arc knot L is presented by the projection image $\lambda_{u_y}(L)$ in the zx plane together with y-coordinate information such that the vertex coordinates $(z,x)^y$ of L ordered from the starting point s are given by

$$(0,0)^0,(0,1)^1,(1,2)^3,(-1,3)^1,(2,1)^{-1},(1,-1)^0,(0,1)^2,(0,3)^0.$$

The arc diagram $D(L;u_y)$ obtained from $\lambda_{u_y}(L)$ is illustrated in Fig. 17. In Fig. 17, the chord diagram $C(D(L;u_y))$ and a simplified chord diagram of it are illustrated. A calculation on the numbers of the knotted and unknotted adjoint chord diagrams of the arc diagram $C(D(L;u_y))$ using the simplified chord diagram of $C(D(L;u_y))$ is done in Fig. 18. Thus, we have

$$p(L;u_y)=p(L;-u_y)=p(-L,u_y)=p(-L,-u_y)=(1,0,0,0)$$

by Corollary 3.1, for L is an even arc knot and $D(L;u_y)$ is an inbound chord diagram.

Example C. Consider an even arc knot L in Fig. 19 given by the non-inbound projection image $\lambda_{u_z}(L)$ in the xy plane together with z-coordinate information such that the vertex coordinates $(x,y)^z$ of L ordered from the starting point s are

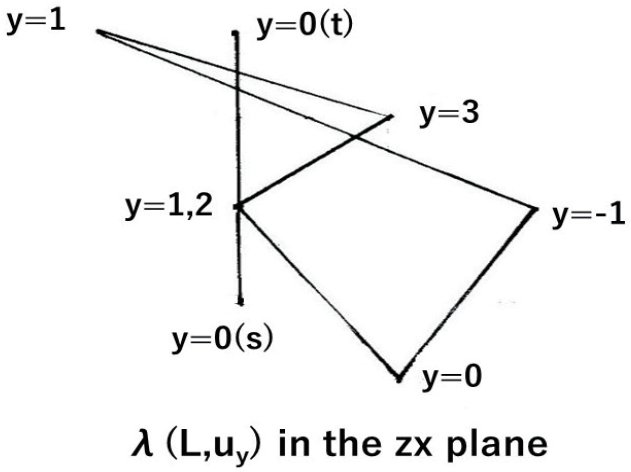

FIGURE 16. The spatial arc L given by the vertex coordinate data: namely, the (z, x) vertex coordinates $(0,0), (0,1), (1,2), (-1,3), (2,1), (1,-1), (0,1), (0,3)$ of $\lambda_{u_y}(L)$ in the zx plane and the y vertex coordinate data in the figure.

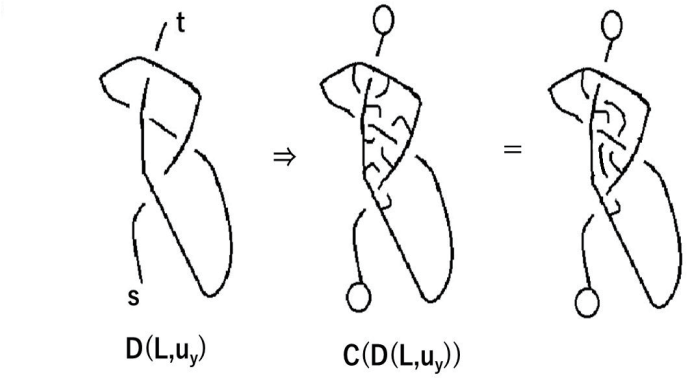

FIGURE 17. Producing the arc diagram $D(L; u_y)$, the chord diagram $C(D(L; u_y))$ and a simplified chord diagram from the projection image $\lambda_{u_y}(L)$

given by

$$(0,0)^0, (1,1)^0, (2,3)^1, (3,1)^{-1}, (1,-1)^{-1}, (-1,0)^1, (1,2)^0, (3,0)^0.$$

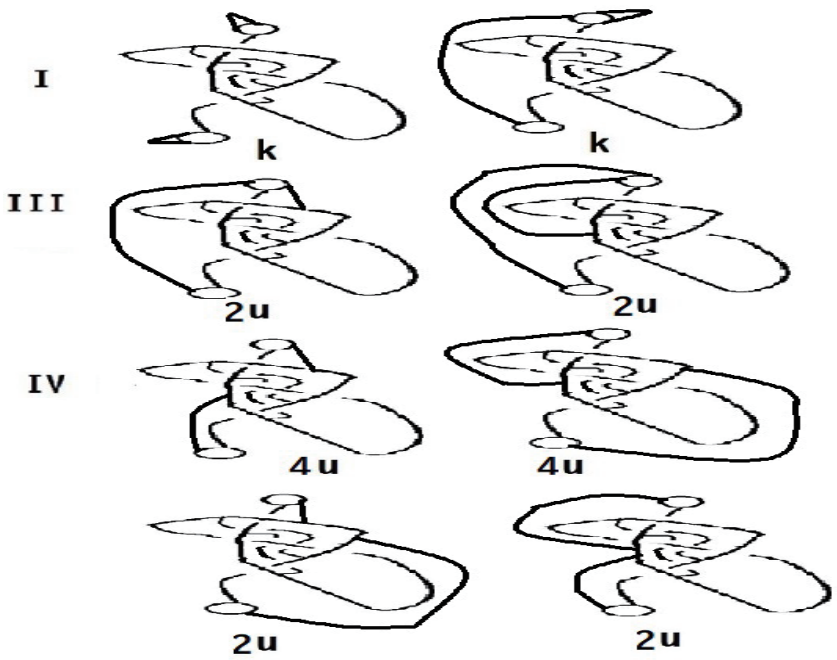

FIGURE 18. Calculations on the chord diagram $C(D(L;u_y))$

Note that the closed knot $\mathrm{cl}(L)$ is a trivial knot. The arc diagram $D(L;u_z)$ coincides with the arc diagram $D(L;u_z)$ in Example B. Thus, we have

$$p(L;u_z) = p(-L,-u_z) = (\frac{1}{2},\frac{1}{2},0,\frac{1}{2}), \quad p(L;-u_z) = p(-L,u_z) = 0.$$

This means that even if the closed knot $\mathrm{cl}(L)$ of an even arc knot L is a trivial knot, the knotting probability $p(L;u)$ may not be zero for a general unit vector u.

In Fig. 20, the same arc knot L is presented by the projection image $\lambda_{u_x}(L)$ in the yz plane together with x-coordinate information such that the vertex coordinates $(y,z)^x$ of L ordered from the starting point s are given by

$$(0,0)^0, (1,0)^1, (3,1)^2, (1,-1)^3, (-1,-1)^1, (0,1)^{-1}, (2,0)^1, (0,0)^3.$$

The arc diagram $D(L;u_x)$ obtained from $\lambda_{u_x}(L)$ is illustrated in Fig. 21 and is an inbound arc diagram whose under-closed knot diagram $\mathrm{cl}_u(D(L;u_x))$ (that is, a knot diagram obtained from $D(L;u_x)$ by joining the endpoints with an under-arc) represents a trivial knot. By [**10**], we have

$$p(L;u_x) = p(L;-u_x) = p(-L,u_x) = p(-L,-u_x) = 0.$$

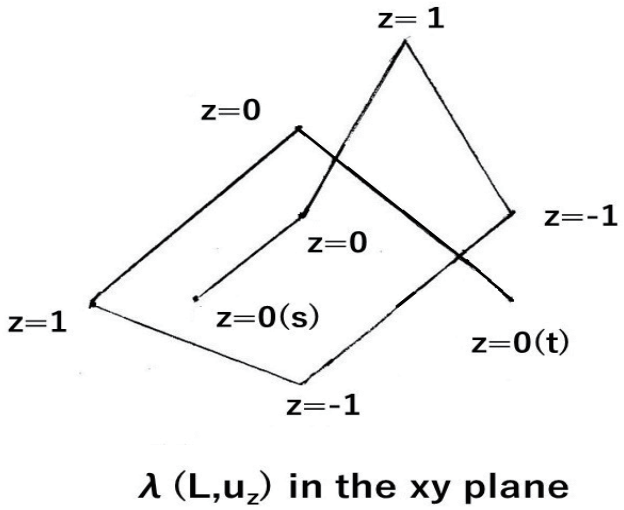

FIGURE 19. The spatial arc L given by the vertex coordinate data: namely, the (x, y) vertex coordinates $(0,0),(1,1),(2,3),(3,1),(1,-1),(-1,0),(1,2),(3,0)$ of $\lambda_{u_z}(L)$ in the xy plane and the z vertex coordinate data in the figure.

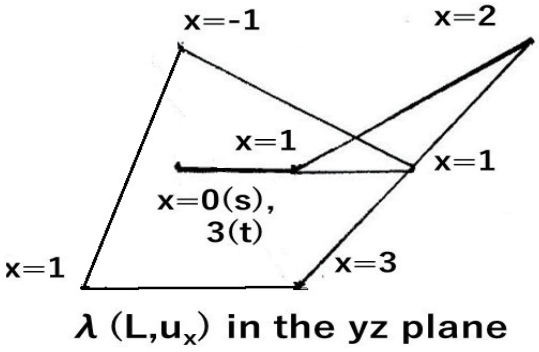

FIGURE 20. The spatial arc L given by the vertex coordinate data: namely, the (y, z) vertex coordinates $(0,0),(1,0),(3,1),(1,-1),(-1,2),(0,1),(2,0),(0,0)$ of $\lambda_{u_x}(L)$ in the yz plane and the x vertex coordinate data in the figure.

In Fig. 22, the same arc knot L is presented by the projection image $\lambda_{u_y}(L)$ in the zx plane together with y-coordinate information such that the vertex coordinates $(z, x)^y$ of L ordered from the starting point s are given by

$$(0,0)^0,(0,1)^1,(1,2)^3,(-1,3)^1,(-1,1)^{-1},(1,-1)^0,(0,1)^2,(0,3)^0.$$

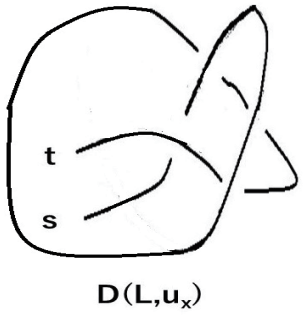

FIGURE 21. Producing the arc diagram $D(L; u_x)$

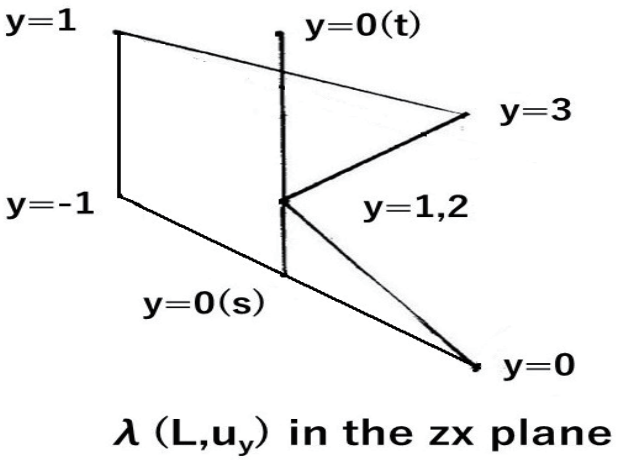

FIGURE 22. The spatial arc L given by the vertex coordinate data: namely, the (z, x) vertex coordinates $(0,0), (0,1), (1,2), (-1,3), (2,1), (1,-1), (0,1), (0,3)$ of $\lambda_{u_y}(L)$ in the zx plane and the y vertex coordinate data in the figure.

The arc diagram $D(L; u_y)$ obtained from $\lambda_{u_y}(L)$ is illustrated in Fig. 23 and isomorphic to the inbound arc diagram in [**10**, Example 4.5] with the knotting probability calculated. Thus, we have

$$p(L; u_y) = p(L; -u_y) = p(-L, u_y) = p(-L, -u_y) = (1, \frac{1}{3}, \frac{1}{3}, 0)$$

Acknowledgements. This work was in part supported by Osaka City University Advanced Mathematical Institute (MEXT Joint Usage/Research Center on Mathematics and Theoretical Physics).

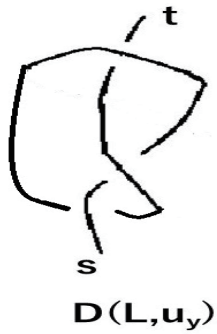

FIGURE 23. Producing the arc diagram $D(L; u_y)$

References

[1] R. H. Crowell and R. H. Fox, Introduction to knot theory (1963) Ginn and Co.; Re-issue Grad. Texts Math., 57 (1977), Springer Verlag.
[2] T. Deguchi and T. Tsurusaki, A statistical study of random knotting using the Vassiliev invariants, J. Knot Theory Ramifications, 3 (1994), 321-353.
[3] A. Kawauchi, A survey of knot theory, Birkhäuser (1996).
[4] A. Kawauchi, On transforming a spatial graph into a plane graph, Statistical Physics and Topology of Polymers with Ramifications to Structure and Function of DNA and Proteins, Progress of Theoretical Physics Supplement, 191 (2011), 235-244.
[5] A. Kawauchi, A chord diagram of a ribbon surface-link, J. Knot Theory Ramifications, 24 (2015), 1540002 (24pp.).
[6] A. Kawauchi, Knot theory for spatial graphs attached to a surface, Contemporary Mathematics, 670 (2016), 141-169.
[7] A. Kawauchi, Supplement to a chord diagram of a ribbon surface-link, J. Knot Theory Ramifications, 26 (2017), 1750033 (5pp.).
[8] A. Kawauchi, A chord graph constructed from a ribbon surface-link, Contemporary Mathematics, 689 (2017), 125-136. Amer. Math. Soc., Providence, RI, USA.
[9] A. Kawauchi, Faithful equivalence of equivalent ribbon surface-links, J. Knot Theory Ramifications, 27, No. 11 (2018),1843003 (23 pages).
[10] A. Kawauchi, Knotting probability of an arc diagram.
http://www.sci.osaka-cu.ac.jp/ kawauchi/diagramknottingprobability.pdf
[11] A. Kawauchi, T. Shibuya and S. Suzuki, Descriptions on surfaces in four-space, I : Normal forms, Math. Sem. Notes, Kobe Univ., 10(1982), 75-125; II: Singularities and cross-sectional links, Math. Sem. Notes, Kobe Univ. 11(1983), 31-69.
[12] , K. Millett, A. Dobay and A. Stasiak, Linear random knots and their scaling behavior, Macromolecules, 38, (2005) 601-606.
[13] E. Uehara and T. Deguchi, Knotting probability of self-avoiding polygons under a topological constraint, J. Chemical Physics, 147, 094901 (2017).
[14] T. Yanagawa, On ribbon 2-knots; the 3-manifold bounded by the 2-knot, Osaka J. Math., 6 (1969), 447-164.

OSAKA CITY UNIVERSITY ADVANCED MATHEMATICAL INSTITUTE, SUGIMOTO, SUMIYOSHI-KU, OSAKA 558-8585, JAPAN
E-mail address: kawauchi@sci.osaka-cu.ac.jp